Kadonaga, *Annu. Rev. Biochem.* **63**, 265 (1994).
2. S. Weisbrod and H. Weintraub, *Proc. Natl. Acad. Sci. U.S.A.* **76**, 630 (1979); M. Bustin *et al.*, *Biochim. Biophys. Acta* **1049**, 231 (1990).
3. Dissenting viewpoints have also been presented: R. H. Nicolas, C. A. Wright, P. N. Cockerill, J. A. Wyke, G. J. Goodwin, *Nucleic Acids Res.* 11, 753 (1983); R. L. Seale, A. T. Annunziato, R. D. Smith, *Biochemistry* **22**, 5008 (1983); A. Stein and T. Townsend, *Nucleic Acids Res.* 11, 6803 (1983); P. S. Swerdlow and A. Varshavsky, *ibid.*, p. 387.
4. S. C. Albright *et al.*, *J. Biol. Chem.* **255**, 3673 (1980); J. K. W. Mardian *et al.*, *Science* **209**, 1534 (1980); G. Sandeen *et al.*, *Nucleic Acids Res.* **8**, 3757 (1980).
5. E. W. Johns, Ed., *The HMG Chromosomal Proteins* (Academic Press, New York, 1982).
6. J. M. Pash, P. J. Alfonso, M. Bustin, *J. Biol. Chem.* **268**, 13632 (1993).
7. M. P. Crippa *et al.*, *EMBO J.* **12**, 3855 (1993).
8. S. C. Batson, R. Sundseth, C. V. Heath, M. Samuels, U. Hansen, *Mol. Cell. Biol.* **12**, 1639 (1992).
9. S. C. Batson, S. Rimsky, R. Sundseth, U. Hansen, *Nucleic Acids Res.* **21**, 3459 (1993).
10. Expression of human HMG-14 mRNA in CV-1 cells. Full-length cDNA for human HMG-14 from pSVL14s (*17*) was inserted at the Bam HI site in the mammalian expression vector pLEN (*18*) to construct pLEN14s. CV-1 cells were transfected through the $CaCl_2$ procedure (*19*) with pLEN14s (20 μg) and pCMV-Neo (1 μg) (*20*). The cells were washed twice 16 hours later with serum-free Dulbecco's modified Eagle's medium (DMEM) and grown in DMEM with 10% calf serum. The cells were split 36 hours after transfection and grown in selective medium [DMEM, 10% calf serum, G418 (1 mg/ml)]. Two to three weeks later, G418-resistant cells were harvested and analyzed for the expression of human HMG-14 mRNA.
11. Simian virus 40 MCs were isolated by extraction from nuclei and purified by sucrose gradient centrifugation as described (*8*). To isolate SV40 viral DNA, confluent plates of CV-1 cells were infected with SV40 at 10 plaque-forming units per cell. At 48 hours after infection, the viral DNA was isolated from cells lysed with 0.6% SDS and 1 M CsCl (*21*) and banded twice in CsCl isopycnic gradients.
12. Unless indicated elsewhere, each reaction mixture contained MCs (DNA content of 200 μg) or SV40 viral DNA (200 μg), pFLBH DNA (50 μg), and poly[*d*(I-C)]·poly[*d*(I-C)] (200 μg). All of the in vitro transcription reactions were performed as outlined at the bottom of each figure, with the use of a preincubation pulse-chase protocol with incubations at 30°C (*8, 22*). HeLa whole-cell extract (WCE) (*23*) provided all the necessary transcription factors. Nucleotide concentrations to label the RNAs during the pulse were 2 μM [α-^{32}P]-uridine 5′-triphosphate (UTP) (20 μCi) and 30 μM of the three unlabeled nucleoside triphosphates. Nucleotide concentrations to chase the transcripts into longer products were 1 mM for UTP and 330 μM for the three remaining nucleoside triphosphates. Specifically initiated RNAs were selected by hybridization with single-stranded M13-SV40 and M13-adenovirus recombinant DNA probes and trimmed by ribonuclease T1 digestion. Probe-1 and probe-2 are single-stranded M13-SV40 recombinant DNAs that contain the late template strand of the SV40 genome from positions 4770 to 874 and 294 to 1782, respectively. These probes lead to the generation of T1-resistant transcripts from the major late SV40 promoter (L325) of 549 nucleotides and 1457 nucleotides, respectively. The probe for SV40 early transcripts contains the early template strand of the SV40 genome from positions 874 to 4770, which leads to the generation of T1-resistant transcripts of 468 to 473 and 510 to 512 nucleotides from the EE and LE promoters, respectively. The resulting T1-resistant transcripts were resolved by 8.3 M urea–5% polyacrylamide gel electrophoresis and analyzed by ImageQuant software on a PhosphorImager (Molecular Dynamics). The numbers for the fold activation by HMG-14 were obtained after correcting for the level of transcripts from the internal control promoters (EE_m or Ad MLP). They were then normalized to levels of transcripts from MCs isolated form parental cells or from SV40 viral DNA in the absence of exogenous HMG-14. Thus, the fold activation for MC or viral DNA in the absence of exogenous HMG-14 is 1.0.
13. M. Bustin *et al.*, *Nucleic Acids Res.* **19**, 3115 (1991).
14. H.-F. Ding and U. Hansen, unpublished data.
15. M. G. Izban and D. S. Luse, *Genes Dev.* **5**, 683 (1991).
16. D. S. Ucker and K. R. Yamamoto, *J. Biol. Chem.* **259**, 7416 (1984).
17. C. Giri *et al.*, *ibid.* **262**, 9839 (1987).
18. G. L. Greene *et al.*, *Science* **231**, 1150 (1986); B. S. Rosen *et al.*, *ibid.* **244**, 1483 (1989).
19. F. M. Ausubel *et al.*, Eds., *Current Protocolsin Molecular Biology* (Greene and Wiley Interscience, New York, 1989).
20. C. Tomasetto, M. J. Neveu, J. Daley, P. K. Horan, R. Sager, *J. Cell Biol.* **122**, 157 (1993).
21. B. Hirt, *J. Mol. Biol.* **26**, 365 (1967).
22. A. Fire, M. Samuels, P. A. Sharp, *J. Biol. Chem.* **259**, 2509 (1984).
23. J. L. Manley *et al.*, *Proc. Natl. Acad. Sci. U.S.A.* **77**, 3855 (1980).
24. M. Bustin, M. P. Crippa, J. M. Pash, *J. Biol. Chem.* **265**, 20077 (1990).
25. M. Samuels *et al.*, *ibid.* **257**, 14419 (1982).
26. We thank J. Licht for aiding in the isolation of stable cell lines and T. White for providing pLEN. Supported by grants from the NIH (GM-36667), the Sandoz/Dana-Farber Cancer Institute Drug Discovery Program, the American Cancer Society (#FRA-415) (U.H.), and Le Fondation pour la Recherche Médicale (S.R.).

1 November 1993; accepted 14 June 1994

Control of Topographic Retinal Axon Branching by Inhibitory Membrane-Bound Molecules

Adina L. Roskies and Dennis D. M. O'Leary*

Retinotopic map development in nonmammalian vertebrates appears to be controlled by molecules that guide or restrict retinal axons to correct locations in their targets. However, the retinotopic map in the superior colliculus (SC) of the rat is developed instead by a topographic bias in collateral branching and arborization. Temporal retinal axons extending across alternating membranes from the topographically correct rostral SC or the incorrect caudal SC of embryonic rats preferentially branch on rostral membranes. Branching preference is due to an inhibitory phosphatidylinositol-linked molecule in the caudal SC. Thus, position-encoding membrane-bound molecules may establish retinotopic maps in mammals by regulating axon branching, not by directing axon growth.

Most axonal connections in the central nervous system are organized in a precise topographic manner. The projection of retinal ganglion cell axons to the optic tectum in nonmammalian vertebrates, or to the homologous SC in mammals, is widely used to investigate mechanisms that control the development of topographic connections. In a mature projection, the temporal-nasal axis of the retina maps along the rostral-caudal axis of the target. In vivo and in vitro studies support the hypothesis that a position-dependent expression of molecules in the retina and its target, in either graded or restricted distributions, governs the topographic targeting of retinal axons (*1*). For example, in vivo studies in developing frogs, fish, and chicks have shown that retinal axons are guided or restricted to their topographically appropriate part of the tectum (*2*). Compelling in vitro evidence for the action of position-encoding molecules comes from the membrane stripe assay, in which temporal retinal axons extending on alternating lanes of membrane from the rostral and caudal tectum prefer to grow on rostral lanes (*3–5*). This growth preference is due to a repulsive phosphatidylinositol (PI)-anchored molecule preferentially associated with the caudal tectum, which is thought to act in vivo by restricting growing temporal retinal axons to their topographically appropriate positions (*4, 6–8*).

Different mechanisms are emphasized in the development of the rat retinocollicular projection (*9, 10*). At embryonic ages, temporal and nasal retinal axons show no distinction in their topographic targeting across the rostral-caudal SC axis (*9*). However, when tested in the membrane stripe assay at these ages, temporal retinal axons show the same strong preference for rostral membrane lanes that chick and fish axons do (*9*). Taken together, these findings indicate that position-dependent information is present in the embryonic SC, but this information does not guide or restrict the growth of retinal axons in vivo. The first observed indication of topographic specificity in the retinocollicular projection is a bias in the distribution of side branches extending from retinal axons that have already grown past their correct topographic locations—temporal axons preferentially branch in the rostral SC and nasal axons in the caudal SC (*9*). A likely role, then, for

Molecular Neurobiology Laboratory, The Salk Institute, 10010 North Torrey Pines Road, La Jolla, CA 92037, USA.

*To whom correspondence should be addressed.

position-encoding molecules in retinocollicular development is in the control of preferential branching and arborization.

We used a modification of the membrane stripe assay to test whether molecules expressed in a position-dependent fashion in the SC govern the topographic branching and arborization of retinal axons. Explants of temporal or nasal retina were cultured on narrow alternating lanes of membranes prepared from the rostral or caudal SC of rats at embryonic day 18 (*11*). Instead of orienting explants so that axons grew parallel to the lanes, as in the typical stripe assay in which axonal growth preference is assessed, we oriented the explants so that axons grew perpendicular to the lanes, repeatedly contacting both rostral and caudal SC membrane lanes (Fig. 1). Axonal branching was assessed after 48 to 72 hours in culture.

When visualized with anterograde axonal tracing with DiI (1,1′-dioctadecyl-3,3,3′,3′-tetramethylindocarbocyanine perchlorate) (Fig. 1A) (*12*) or by staining with a vital dye (Fig. 1C) (*13*), it was apparent that both temporal and nasal axons extended branches on the membrane carpets (*14, 15*). Temporal axons appeared to branch more on the topographically appropriate rostral lanes than on the topographically inappropriate caudal lanes in 61 of 63 cases (*16*). This preference was observed whether the rostral SC membranes were laid down first or second. Visual inspection of 20 cases of nasal explant growth detected no consistent branching preference (*17, 18*).

To verify these qualitative impressions of branching preference, we used two methods of quantification: "anterograde" and "retrograde" (Fig. 2A). Anterograde quantification allowed us to acquire data from the full field of neuronal outgrowth. For this method, the entire axonal plexus was labeled by DiI injections into the explant (*12*) or by vital dye staining (*13*). Retrograde quantification allowed us to identify branches unambiguously. For this method, cultures were fixed and a small deposit of DiI was placed distal to the explant (Fig. 1, D through F) (*19*). Both quantification methods demonstrated that temporal axons consistently branched more on rostral lanes than on caudal lanes (Fig. 2B). In contrast, nasal axons showed no consistent branching preference for either set of lanes (Fig. 2B).

These findings demonstrate that the in vitro specificity of temporal axon branching is governed by membrane-bound molecules that are differentially distributed in the SC. To determine whether a PI-linked molecule controls this topographic bias in branching, as it does the growth preference of temporal axons for rostral tectal membranes in chicks (*4, 7*), we treated different combinations of the SC membrane suspensions with a PI-specific phospholipase C (PI-PLC), an enzyme that selectively cleaves the PI linkage (*20*). As a control, we first established that a repulsive PI-linked molecule associated with caudal SC membranes was responsible for the growth preference of temporal retinal axons for rostral SC membranes in rats. This growth preference was abolished when caudal SC membranes were treated with PI-PLC (n = 15) (Fig. 3, A and B) and when both rostral and caudal SC membranes were treated (n = 1). When caudal SC membranes were treated with PI-PLC in the branching assay, we found that temporal axons branched well on both rostral and treated caudal lanes (n = 30) (Fig. 3C). Quantification of branching showed that the branching preference was abolished by PI-PLC treatment of caudal SC membranes (Fig. 4). Treatment of both rostral and caudal SC membranes also abolished the branching preference of temporal axons (n = 1), whereas treatment of only rostral SC membranes did not (n = 2). These findings indicate that the branching specificity of temporal axons is due to the inhibitory activity of a PI-linked molecule that is associated with caudal SC membranes.

In some instances, we observed complex "arborlike" structures on the membrane carpets. In the normal branching assay, all such arbors formed by temporal axons were restricted to the rostral lanes (n = 29) (Figs. 1B and 3D). When observed on carpets in which caudal lanes had been pretreated with PI-PLC, the arborlike structures formed by temporal axons often bridged lane boundaries (in two out of three cases) (Fig. 3E). Thus, an inhibitory PI-linked molecule associated with caudal SC membranes appears to restrict the arborlike structures formed by temporal axons to rostral lanes.

Our in vitro findings indicate that a membrane-associated molecule controls the branching specificity of temporal retinal axons, that this molecule is preferentially distributed in the caudal SC, that it is PI-linked to the cell membrane, and that it acts by means of inhibition. By analogy to in vivo observations (*9*), we suspect that the branches observed in vitro form interstitially along the axon, but we cannot exclude the possibility that branches also

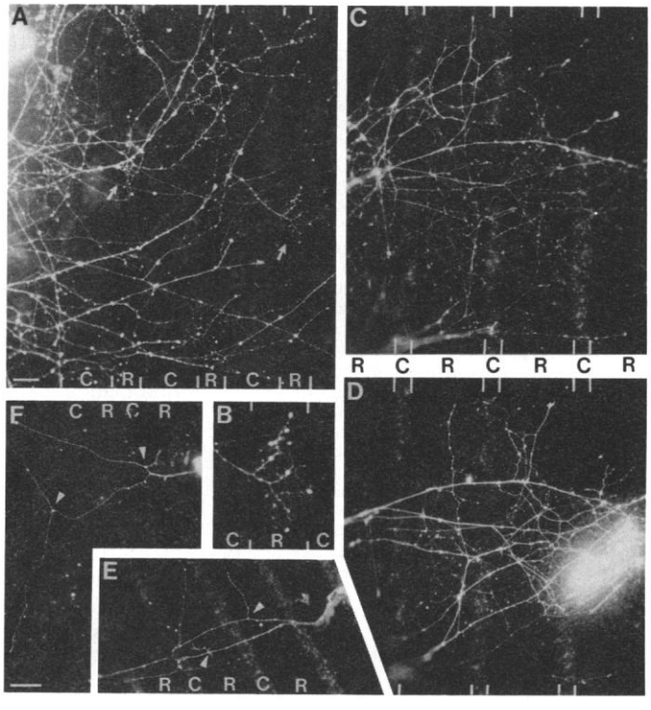

Fig. 1. Temporal retinal axons prefer to branch on rostral SC membranes. All photos are double exposures to show caudal SC membrane lanes marked by latex microspheres (in all figures, rostral lanes are indicated by R, caudal lanes by C). Explants are to the left, out of view. (**A**) Temporal neurites on an alternating carpet of rostral and caudal SC membrane lanes; caudal SC membranes were laid down first and rostral SC membranes second. Axons were anterogradely labeled by DiI injected into the retinal explant after fixation (*12*). As is typical, temporal axons show minimal branching on caudal lanes and substantial branching on rostral lanes. Two examples of profuse branching on rostral lanes are marked with arrows. (**B**) Higher power view of profuse branching on rostral lanes denoted by an arrow in (A). (**C** and **D**) Temporal axons growing on carpets in which rostral SC membranes were laid down first. In (C), neurites are labeled with a vital dye (*13*); (D) shows the same field as (C), in which a proportion of the axons visualized with the vital dye in (C) were retrogradely labeled with a deposit of DiI (large white mass) made distally along the axonal outgrowth (*19*). With both labeling methods, the preference for temporal axons to branch on rostral lanes is evident. (**E** and **F**) Isolated temporal axons on carpets with rostral SC membranes laid down first (E) or second (F). In each example, axons were retrogradely labeled with small DiI deposits at the right edge of the photos. In both cases, branches were found only on rostral lanes; some branch points are marked by arrowheads. Scale bar in (A): 50 μm in (A), (C), and (D); 25 μm in (B). Scale bar in (F): 100 μm in (E) and (F).

form by growth cone bifurcation. Branch specificity could be generated by the inhibitory activity affecting either branch initiation or stabilization: The initiation of branching could be curtailed along the segment of axon that is in contact with the inhibitory molecule; alternatively, branch initiation may not be affected, but the inhibitory molecule may promote the withdrawal of branches that form along the segment of axon that is in contact with it. Cox *et al.* (*21*) have shown that chick caudal tectal membranes applied to retinal axon growth cones in vitro cause the selective collapse of temporal axon growth cones [also see (*22*)]. The related activity that we have identified in the rat caudal SC could act on temporal retinal axons through a similar mechanism, either early in the process of branch formation, to prevent branch initiation, or later, after branches form, to prevent branch stabilization (*23*).

In contrast, a trophic mechanism for establishing topographic specificity in the retinotectal system has been suggested by von Boxberg *et al.* (*24*), who demonstrated that the survival of chick nasal retinal axons in long-term cultures is promoted by the binding of protein-enriched reconstituted vesicles from the caudal tectum. It is possible that the trophic effect of the tectal vesicles is a local one, able to promote retention of correctly positioned branches without stabilizing incorrectly positioned branches formed by the same parent axon. Thus, two distinct mechanisms, one based

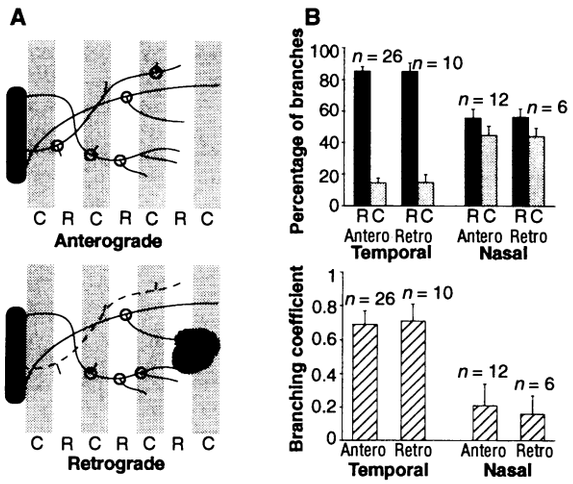

Fig. 2. Quantification of branching preferences. (**A**) Quantification scheme. Two methods of branch quantification, "anterograde" and "retrograde," were used. Counts of axonal branches were binned for each set of membrane lanes and were normalized for differences in relative lane width. Retinal explants are indicated by the black ovals. Circles mark intersections between labeled processes that met criteria to be scored as branches (described below). (**Top**) Anterograde labeling. Neurites >5 μm in length and extending at approximately right angles from other neurites were scored as branches. Instances in which neurites intersect and both processes clearly extend beyond the intersection were excluded from counts. These criteria minimized the misidentification of defasciculating or crossing axons as branches; nonetheless, anterograde labeling of axons does not unambiguously distinguish branches from splitting fascicles. (**Bottom**) Retrograde labeling. To identify branches unambiguously, we used retrograde labeling. Labeled processes >5 μm in length and proximal to a DiI deposit (black cloud) but not contacting the deposit, which extend from DiI-labeled axons that do contact the DiI deposit, were scored as branches. The dashed axon is one that would be anterogradely labeled but not retrogradely labeled. (**B**) Histograms of branching data. (**Top**) Data from perpendicular stripe assays showing the percentage of branches from temporal and nasal axons on rostral and caudal lanes with the use of anterograde (antero) and retrograde (retro) quantification; 85.4% of branches formed by temporal axons were found on rostral lanes; nasal axons showed no consistent preference. (**Bottom**) The same data expressed as a branching coefficient: bc = [(number of branches on rostral lanes) − (number of branches on caudal lanes)]/(total branches). A branching coefficient of 1 represents a complete preference for rostral lanes, and a coefficient of 0 represents no preference. For temporal neurite preference for rostral lanes $P \ll 0.0005$; for nasal neurites showing the same preference as temporal neurites $P < 0.0005$ (retro) and $P < 0.0025$ (antero).

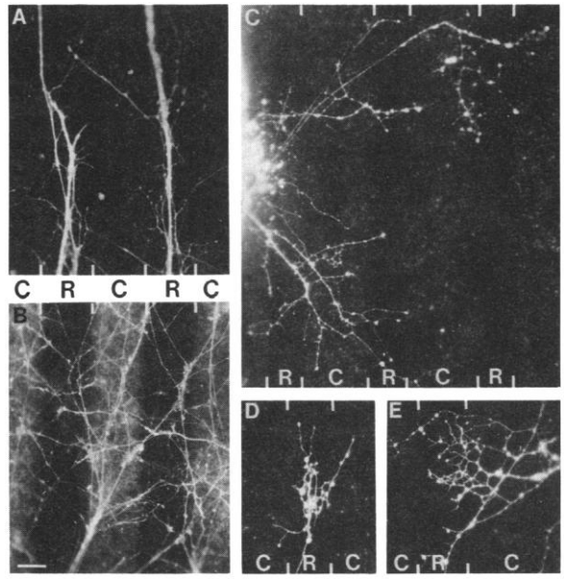

Fig. 3. Branching specificity of temporal axons was eliminated by treatment of caudal SC membranes with PI-PLC. (**A** and **B**) Temporal neurites grown parallel to alternating lanes of rostral and caudal SC membranes; explants are off the bottom of the photos. In (A), temporal axons show a strong preference for rostral lanes; axons were anterogradely labeled with DiI (*12*). In (B), the growth preference of temporal axons for rostral lanes was abolished by treatment of caudal SC membranes with PI-PLC; axons were stained with a vital dye (*13*). (**C**) Temporal axons growing perpendicular to SC membrane lanes on a carpet in which caudal lanes were pretreated with PI-PLC; temporal axons branch well on caudal lanes and show no preference for branching on rostral lanes. Explant is out of view to the left. (**D**) An example of an arborlike structure restricted to a rostral lane. (**E**) An arborlike structure on a carpet in which caudal SC membranes were treated with PI-PLC. The arbor extends across a set of rostral and caudal lanes. In (C) through (E), axons were anterogradely labeled with DiI (*12*). Scale bar in (B): 50 μm in (A), (B), and (C); 40 μm in (D); and 35 μm in (E).

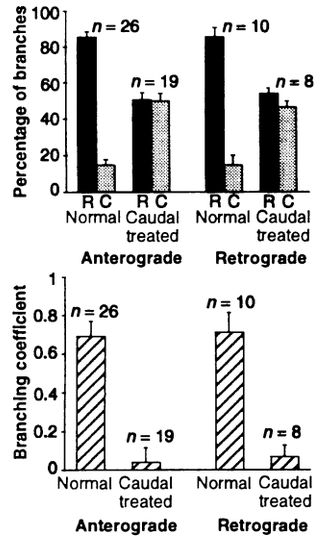

Fig. 4. Quantification of temporal axon branching on normal membrane carpets and on carpets with PI-PLC–treated caudal SC membranes. (**Top**) The percentage of branches observed on rostral and caudal membrane lanes in normal (as in Fig. 2) and caudal PI-PLC–treated cases. The strong branching preference normally seen is abolished when the caudal SC membranes are treated with PI-PLC. Both anterograde and retrograde quantification yield similar results. For all measures, $P \ll 0.0005$. (**Bottom**) The same data presented as branching coefficients. A branching coefficient of 1 represents a complete preference for rostral lanes; 0 indicates no preference for either set of lanes.

on inhibition or repulsion and one based on trophism, which act on separate populations of retinal axons, may complement each other in establishing topographic specificity.

In vitro studies in fish (*5*), frogs (*25*), chicks (*3, 4, 6*), and rodents (*9, 26*) indicate that a molecule present on the surfaces of cells in the caudal tectum and the caudal SC, which inhibits or repulses the growth of temporal retinal axons, is conserved across vertebrate species. It has been hypothesized that this molecule governs retinal axon targeting. In rats, the preferential branching of retinal axons at topographically appropriate locations in the SC, rather than directed retinal axon growth, appears to be a crucial event in the establishment of retinotopic connections (*9*). Our findings show that this inhibitory molecule controls topographic branching specificity in vitro and therefore suggest that this molecule may act in the same manner in vivo to regulate the topographic specificity of retinal axon branching that is evident in the developing SC. The topographic bias in the distribution of collateral branches could then serve as the framework for subsequent molecular and activity-dependent mechanisms that control axon pruning and synaptic stabilization (*27*). This means of establishing topographically ordered synaptic connections shifts the emphasis from axon guidance and growth cone behavior to events that occur along the axon shaft, which result in the development of collateral branches. Thus, a cascade of events, beginning with selective axon branching, appears to drive the refinement of an initially coarse map into one with the topographic precision required for the processing of sensory information in the central nervous system.

REFERENCES AND NOTES

1. R. W. Sperry, *Proc. Natl. Acad. Sci. U.S.A.* **50**, 703 (1963); F. Bonhoeffer and A. Gierer, *Trends Neurosci.* **7**, 378 (1984); A. Gierer, *Development* **101**, 479 (1987); S. Udin and J. W. Fawcett, *Annu. Rev. Neurosci.* **11**, 289 (1988); S. E. Fraser, *Curr. Opin. Neurobiol.* **2**, 83 (1992); D. D. M. O'Leary and D. K. Simon, *Semin. Neurosci.* **4**, 365 (1992); J. R. Sanes, *Curr. Opin. Neurobiol.* **3**, 67 (1992); C. E. Holt and W. A. Harris, *J. Neurobiol.* **24**, 1400 (1993).
2. Frogs: C. E. Holt and W. A. Harris, *Nature* **301**, 150 (1983); D. S. Sakaguchi and R. K. Murphey, *J. Neurosci.* **5**, 3228 (1985); W. A. Harris, *Nature* **339**, 218 (1989); H. Fujisawa, *Dev. Growth Differ.* **26**, 545 (1984); *J. Comp. Neurol.* **260**, 127 (1987). Fish: C. A. O. Stuermer, *J. Neurosci.* **8**, 4513 (1988); E. Cornel and C. Holt, *Neuron* **9**, 1001 (1992); but also see N. A. O'Rourke and S. E. Fraser, *Dev. Biol.* **114**, 265 (1986); *Neuron* **5**, 159 (1991). Chicks: S. Thanos and F. Bonhoeffer, *J. Comp. Neurol.* **224**, 407 (1983); *ibid.* **261**, 155 (1987). Recent studies in chicks have reported that growing temporal axons are restricted to the rostral tectum, but within the rostral tectum, these axons overshoot their topographically correct locations. Topographically ordered arbors are later established through the extension of collateral branches [H. Nakamura and D. D. M. O'Leary, *J. Neurosci.* **9**, 3776 (1989); K. Matsui and D. D. M. O'Leary, *Soc. Neurosci. Abstr.* **15**, 1212 (1989)].
3. J. Walter, B. Kern-Veits, J. Huf, B. Stolze, F. Bonhoeffer, *Development* **101**, 685 (1987).
4. H. Baier and F. Bonhoeffer, *Science* **255**, 472 (1992).
5. J. Vielmetter and C. A. O. Stuermer, *Neuron* **2**, 1331 (1989).
6. J. Walter, S. Henke-Fahle, F. Bonhoeffer, *Development* **101**, 909 (1987).
7. J. Walter, B. Muller, F. Bonhoeffer, *J. Physiol. (Paris)* **84**, 104 (1990).
8. B. Stahl, B. Muller, Y. von Boxberg, E. Cox, F. Bonhoeffer, *Neuron* **5**, 735 (1990).
9. D. K. Simon and D. D. M. O'Leary, *ibid.* **9**, 1 (1992).
10. ———, *J. Neurosci.* **12**, 1212 (1992); A. L. Roskies and D. D. M. O'Leary, *Soc. Neurosci. Abstr.* **18**, 222 (1992).
11. For all assays, fetuses at embryonic day (E) 18 were removed from anesthetized, timed pregnant Sprague-Dawley rats. E0 refers to day of insemination. The stripe assay was done as described in (*3*) and (*9*). The SCs were dissected, and the overlying pia and underlying white matter were removed. Rostral and caudal SC halves were homogenized separately in buffer [10 mM tris-Cl (pH 7.4) and 1.5 mM $CaCl_2$] with protease inhibitors [200 IU of aprotinin per milliliter, 50 μM leupeptin, 2 μM pepstatin, 1 mM spermidine, and 50 μM 2,3-dehydro-2-deoxy-*N*-acetylneuraminic acid (Sigma)]. Membranes were fractionated by centrifugation in a sucrose gradient and washed and resuspended in phosphate-buffered saline with protease inhibitors (PBS+). The pellet was resuspended in PBS+ and adjusted so that a 1:15 dilution of the suspension in 2% SDS yielded an optical density of 0.2 when measured with 220-nm ultraviolet (UV) light. Latex microspheres that fluoresce blue when exposed to UV illumination were added to the caudal membrane suspension. Alternating rostral and caudal SC membrane lanes were laid down on a Nuclepore filter (Costar, Cambridge, MA; pore size, 0.1 μm), by means of a microchannel device (*3*) and suction. Retinas were dissected from the sclera and the inner capillary layer was removed. Retinas were mounted on nitrocellulose paper with the ganglion cell layer facing up, and 300-μm strips of temporal and nasal retina were cut on a tissue chopper. Explants were placed on the membrane carpets with the ganglion cell layer facing down, parallel to the membrane lanes and held in place with small weights. Two milliliters of DMEM-F12, supplemented with 0.4% methylcellulose, 2 mM L-glutamine, 0.6% D-glucose, 10 units of pen-strep per milliliter, 10 mM Hepes, 5% rat serum, and 10% fetal bovine serum, were added to each dish. Cultures were incubated in 5% CO_2 at 37°C for 48 to 72 hours before analysis.
12. Cultures were fixed in buffered 4% paraformaldehyde. Anterograde axonal labeling was done by making multiple small DiI (Molecular Probes, Eugene, OR) injections (1 to 5% in dimethylformamide) (Sigma) into the fixed explant with a picospritzer (General Valve, Fairfield, NJ) [P. Godement, H. Vanselow, S. Thanos, F. Bonhoeffer, *Development* **101**, 697 (1987); M. G. Honig and R. I. Hume, *Trends Neurosci.* **12**, 333 (1989)]. Carpets were kept in the dark for 12 to 24 hours, which allowed the dye to diffuse down the axons, and then were analyzed and photographed under rhodamine illumination.
13. The vital dye fluorescein succinamyldiester acetate (FSA) (Molecular Probes) labels all living cells and their processes. For visualizing axonal outgrowth with the vital dye, the culture medium was replaced with a 1:3000 dilution of FSA in phosphate buffer. After 5 min, this solution was washed out with a solution of 5 mM *p*-phenylenediamine in phosphate buffer before fixation in 4% buffered paraformaldehyde [M. Bronner-Fraser, *J. Cell Biol.* **101**, 610 (1985); R. Tuttle and W. Matthew, *J. Neurosci. Methods* **39**, 193 (1991)].
14. Cultures that did not meet several criteria were not further analyzed. These criteria were that the membrane lanes were clearly defined, axons were not heavily fasciculated, and at least three axons had to have grown across three or more lanes (>270 μm). From the pool of cases that met these criteria, a subset was randomly selected for quantification of branching preferences.
15. Explants were also cultured on homogeneous carpets of rostral or caudal SC membranes. Temporal axons branched extensively on homogeneous rostral carpets (n = 17; good growth and branching in 14 cases). However, temporal axons grew poorly on homogeneous carpets of caudal SC membranes (n = 15): In 4 cases, a few axons extended but were highly fasciculated; in 11 cases, temporal explants failed to extend any axons. Nasal explants grew and branched well on homogeneous carpets of both rostral (n = 3) and caudal SC membranes (n = 6). When temporal explants were grown on homogeneous carpets of caudal SC membranes treated with PI-PLC, they grew well and branched as they did on rostral carpets (n = 2) and were indistinguishable from nasal explants on similarly prepared carpets (n = 2). These findings indicate that the contrast between SC membrane types that was provided in the stripe assay is not required for branching. The poor outgrowth of temporal axons on homogeneous carpets of caudal SC membranes as compared to that on rostral SC membranes is similar to findings in fish (*5*) but differs with results seen in chicks, in which temporal axons grow equally well on homogeneous carpets of rostral and caudal tectal membranes (*3*).
16. Of the two temporal cases not showing a preference for rostral lanes, a branching preference could not be distinguished in one case, and in the other case temporal axons appeared to prefer caudal lanes.
17. The first set of lanes laid down was usually wider than the second. For this reason, our data were normalized for lane width. Regardless of which set of membrane lanes was laid down first, temporal axons preferred to branch on rostral lanes. A second-lane artifact was apparent in assays of nasal axon branching. Of 20 cases of nasal axon branching examined, 11 cases showed no discernible branching preference. In the remaining 9 cases, 4 showed a preference for branching on rostral lanes, and 5 showed a preference for caudal lanes; in all of these cases, the preference was for the second set of lanes laid down. A similar artifact affecting nasal axon preference has been reported in studies examining axonal growth preferences by use of the parallel stripe assay (*5, 9, 26*).
18. The absence of a consistent branching preference of nasal axons is in agreement with results from chicks (*3*), fish (*5*), mice (*26*), and rats (*9*) that indicate that nasal axons show no consistent axonal growth preference when given the choice between rostral and caudal tectal-SC membrane lanes in the parallel stripe assay.
19. For retrograde labeling, cultures were fixed with buffered 4% paraformaldehyde, and small deposits of DiI (*12*) were injected onto the surface of the membrane carpet away from the explant by means of a picospritzer. DiI is hydrophobic, and the injections formed discrete deposits on the carpets. Only axons in contact with the DiI deposit, as well as the branches of these axons, were labeled; injections not placed in contact with axons resulted in no axonal labeling. Therefore, labeled processes that did not contact the DiI deposit, but extended from a DiI-labeled axon that did, could be unambiguously identified as a collateral branch. Carpets were photographed 12 to 24 hours after DiI application.
20. The assays were done as before, except that before lane application, the treated membrane suspension was incubated for 1 hour at 37°C in a 10 mM tris-Cl solution (pH 7.4) with protease inhibitors, 10 to 20 μU of PI-PLC per milliliter (from *Bacillus cereus*; Boehringer Mannheim, Mannheim, Germany), and 1 mM 1,10-phenanthroline

(Sigma) (7). Enzyme treatment was stopped by the addition of an equal volume of 2 M KCl in 10 mM tris-Cl. Control membranes were processed in the same way but without the addition of PI-PLC.
21. E. Cox, B. Muller, F. Bonhoeffer, *Neuron* **2**, 31 (1990).
22. Different inhibitory molecules isolated from other developing tissues have also been shown to induce growth-cone collapse in vitro [J. Kapfhammer and J. A. Raper, *J. Neurosci.* **7**, 201 (1987); C. Bandtlow, T. Zachleder, M. E. Schwab, *ibid.* **10**, 3837 (1990); J. A. Davies, G. M. Cook, C. D. Stern, R. J. Keynes, *Neuron* **4**, 11 (1990); Y. Luo, D. Raible, J. A. Raper, *Cell* **75**, 217 (1993)].
23. Inhibition of branch initiation has been hypothesized by Schwab and colleagues to operate in the mature nervous system. They have reported that x-ray irradiation of rat pups to remove oligodendrocytes, which express the inhibitory protein NI-35/250, results in the sprouting of retinal axons in the optic nerve [R. J. Colello and M. E. Schwab, *J. Neurosci.*, in press]. Thus, similar mechanisms may act in developing and maturing nervous systems, first to establish and then to maintain appropriate connectivity.
24. Y. v. Boxberg, S. Deiss, U. Schwarz, *Neuron* **10**, 345 (1993).
25. A. R. Johnston and D. J. Gooday, *Development* **113**, 409 (1991).
26. P. Godement and F. Bonhoeffer, *ibid.* **106**, 313 (1989).
27. H. T. Cline and M. Constantine-Paton, *Neuron* **3**, 413 (1989); C. J. Shatz and M. P. Stryker, *Science* **242**, 87 (1988); M. Constantine-Paton, H. T. Cline, E. Debski, *Annu. Rev. Neurosci.* **13**, 129 (1990); C. J. Shatz, *Neuron* **5**, 745 (1990); P. R. Montague, J. A. Gally, G. M. Edelman, *Cereb. Cortex* **1**, 199 (1991); D. K. Simon, G. T. Prusky, D. D. M. O'Leary, M. Constantine-Paton, *Proc. Natl. Acad. Sci. U.S.A.* **89**, 10593 (1992); C. J. Shatz and C. S. Goodman, *Cell/Neuron* **(suppl.) 72/10**, 77 (1993).
28. Experimental procedures were approved by the Animal Care and Use Committee of the Salk Institute. Supported by NEI grant R01 EY07025. We thank E. Nurmi for technical assistance, F. Bonhoeffer for providing the microchannel device, and M. Daston for helpful comments on the manuscript.

30 March 1994; accepted 6 June 1994

Induction of Mesoderm in *Xenopus laevis* Embryos by Translation Initiation Factor 4E

Peter S. Klein and Douglas A. Melton*

The microinjection of messenger RNA encoding the eukaryotic translation initiation factor 4E (eIF-4E) into early embryos of *Xenopus laevis* leads to the induction of mesoderm in ectodermal explants. This induction occurs without a stimulation of overall protein synthesis and is blocked by the co-expression of a dominant negative mutant of the proto-oncogene *ras* or a truncated activin type II receptor. Although other translation factors have been studied in vertebrate and invertebrate embryos, none have been shown to play a direct role in development. The results here suggest a mechanism for relaying and amplifying signals for mesoderm induction.

Unfertilized eggs contain a large store of maternal mRNAs, many of which are only translated after fertilization (*1*). A number of mechanisms have been described in vertebrates and invertebrates that regulate the translation of these mRNAs (*2*–*6*). For example, primary (such as polyadenylation) structure and secondary structure of mRNA, as well as RNA binding proteins, can affect the efficiency of translation (*4*–*6*). During early embryogenesis, the pattern of regulated mRNAs changes, so that different mRNAs may be recruited to the ribosome at different times in development, as in *Xenopus laevis* embryos (*1*, *7*). Several examples of the translational control of specific mRNAs involved in early developmental processes have been described recently in *Drosophila* and *Caenorhabditis elegans* (*8*), but translational regulation has not been shown to play a direct role in the development of vertebrate embryos.

An early step in embryogenesis is the formation of the primordial germ layers, ectoderm, mesoderm, and endoderm. In *Xenopus laevis*, mesoderm is believed to arise by an inductive signal from vegetal cells of the blastula acting on adjacent cells in the animal hemisphere (*9*). Members of the transforming growth factor (TGF)–β and fibroblast growth factor (FGF) families mimic the endogenous signal when animal pole explants (prospective ectoderm) are cultured in a solution of the respective factor [reviewed in (*10*)]. Activin, FGF, and their receptors are expressed in the embryo, and dominant negative mutants for both receptors either abolish or markedly disrupt the formation of mesoderm in embryos (*11*).

We are interested in whether mesoderm induction in *Xenopus* involves the translational regulation of specific mRNAs. Several translation factors have been studied in oocytes and embryos of *Xenopus*, sea urchins, starfish, and brine shrimp, and over-expression can lead to a modest increase in the rate of total protein synthesis in some cases (*12*). However, these factors have not been shown to regulate developmental processes.

Our initial studies have focused on the translation initiation factor eIF-4E, the mRNA cap-binding protein. This factor appears to be an important control point for the regulation of protein synthesis and cell division [reviewed in (*3*, *13*)]. The overexpression of eIF-4E in NIH 3T3 cells, rat embryonic fibroblasts, and HeLa cells can lead to aberrant growth and oncogenic transformation as determined by growth rate, morphology, focus formation in cell monolayers, and tumor formation in nude mice (*14*, *15*). Transformation by eIF-4E is blocked by a dominant negative mutant of ras (*16*). In addition, eIF-4E appears to be an early downstream target of a number of growth regulatory molecules such as platelet-derived growth factor, epidermal growth factor, tumor necrosis factor, insulin, and others (*3*), all of which induce eIF-4E phosphorylation. These findings have suggested that eIF-4E participates in the ras signal transduction pathway regulating cell division.

To address whether eIF-4E may regulate the translation of mRNAs specifically involved in mesoderm induction, eIF-4E mRNA was micro-injected into the animal pole of one to two cell embryos (*17*). The *Xenopus* translation elongation factor–1α (EF-1α) was injected into a parallel set of embryos to serve as a control (*18*). At the blastula stage [stage 8 to 9 (*19*)], animal caps were dissected and cultured in buffer until siblings had reached the late tail-bud stage. By the late neurula stage, animal caps from embryos injected with eIF-4E mRNA had elongated in a manner similar to that of animal caps treated with FGF or a low dose of activin while caps from embryos injected with EF-1α (as well as uninjected embryos) remained spherical, typical of uninduced ectodermal explants. By the tail-bud stage, the animal caps expressing eIF-4E had formed large vesicles in greater than 90% of cases (80 of 87, Fig. 1), while those expressing EF-1α, as well as uninjected caps, were uninduced (0 of 55). Histological analysis showed that eIF-4E injection had led to the induction of mesenchyme and coelomic cavities lined with mesothelium, while controls showed only atypical epidermis (Fig. 1). A mutated eIF-4E in which Ser-53 has been converted to Ala (*14*, *15*, *17*) also leads to the elongation of ectodermal explants, although in a lower percent (53%, 20 of 38) of cases. This mutant is inactive in cell transformation assays (*14*, *15*), but in some cell types the Ala-53 mutated eIF-4E appears to be functional and highly phosphorylated, suggesting that alternative sites of phosphorylation may be important for regulation in other cell types (*20*). At present, the phosphorylation sites in *Xeno-*

Department of Biochemistry and Molecular Biology, Harvard University, 7 Divinity Avenue, Cambridge, MA 02138, USA.

*To whom correspondence should be addressed.